Wide Area Control of Governors and Power System Stabilizers with an Adaptive Tuning of Coordination Signals

Lazaros Zacharia, *Graduate Student Member, IEEE,* Markos Asprou, *Member, IEEE,* and Elias Kyriakides, *Senior Member, IEEE*

***Abstract*—This paper presents the formulation of Wide Area Control (WAC) signals for either coordinating all the governors of the system or coordinating simultaneously both the governor and the Power System Stabilizer (PSS) of each generator. This is achieved through the development of suitable WAC signals intended for the coordination of their common input signal (rotor speed deviation) having as objective the compensation of all the local and inter-area oscillations. Furthermore, an adaptive tuning method to estimate weights for each inter-generator interaction is also presented. This is required to regulate adaptively the level of the WAC contribution to all the local controllers. The weights are computed according to the electric connectivity between the generators. For the evaluation of the proposed methods, both offline and real-time simulations are performed on the IEEE 39-bus test system. The results indicate the substantial improvement of the system's stability when the proposed governor/PSS coordination is considered. The performance of the WAC scheme is further increased when the adaptive tuning procedure is applied. Finally, the requirement of having PMUs at each generator bus is relaxed by utilizing the coherency concept.**

***Index Terms*—Adaptive tuning, coherency, governor coordination, inter-area oscillation damping, power system stabilizer, real-time simulation, wide area control.**

I. Introduction

Inter-area oscillations have become one of the major challenges that modern power systems have to confront. These oscillations can provide additional stress to the system's components, reduce the power quality and can even threaten the stability of the system [1]. More specifically, the occurrence of any type of contingency during the transfer of large amounts of power between interconnected systems (through long transmission lines), worsens the inter-area oscillations [2]. Inter-area oscillations represent one of the two electromechanical properties of the dynamic power systems. These oscillations are the result of having coherent groups of generators swinging against each other (at the event of a disturbance) and they are characterized by low frequency (0.2-1 Hz) [3]. Due to their nature, they are also known as low-frequency oscillation modes.

Traditionally, the power system oscillations are damped through the generator local controllers, such as the exciter and governor, which are designed to ensure only the local stability of the generator (1-2 Hz). In order to increase the stability of the system, Power System Stabilizers (PSSs) and power electronic converter based Flexible AC Transmission System (FACTS) devices are added in the grid [4], [5]. More specifically, the PSSs are implemented to increase the small-signal stability by generating an electric torque component, which aims to compensate only the local part of the low frequency oscillations [4]. Although the PSSs are utilized for damping the inter-area modes, further improvement can be achieved. The drawback of such a decentralized architecture, is that each local controller (e.g., PSS, FACTS) tries to damp the oscillations based only on local information, ignoring the operation of the other controllers [5]. Therefore, the lack of global information and the absence of a common system objective for all the local controllers provide an opportunity to enhance further the damping of the inter-area oscillations.

The advent and application of synchronized measurement technology has enabled the detection and observation of poorly damped oscillations (such as the inter-area modes) and became the backbone for the development of the Wide Area Monitoring and Control (WAMC) systems [6]. More specifically, Wide Area Control (WAC) aims to utilize the synchronized phasor measurements in order to provide coordination signals to the local controllers, making them capable of damping effectively all the inter-area oscillations [4]. In the literature, various works dealt with the development of a wide area controller. The proposed WAC schemes are segregated mainly according to the components of the power system that the wide area controller is intended to coordinate. For example, in [7] a wide area controller is developed for the modulation of the active power of a high-voltage DC (HVDC) line using synchronized measurements. The authors in [8] formulated a control scheme which obtains wide area information from the system and utilizes doubly-fed induction generator (DFIG) wind farms to damp any oscillations. A combination of controlling synchronous generators and FACTS is presented in [5]. A

This work has been supported in part by the European Union's Horizon 2020 research and innovation programme under grant agreement No 739551 (KIOS CoE) and from the Government of the Republic of Cyprus through the Directorate General for European Programmes, Coordination and Development. This work was also co-funded by the European Regional Development Fund and the Republic of Cyprus through the Research and Innovation Foundation (Project: INTEGRATED/0916/0035).

The authors are with the Department of Electrical and Computer Engineering and the KIOS Research and Innovation Center of Excellence, University of Cyprus, Nicosia, 1678, Cyprus (email: zacharia.lazaros@ucy.ac.cy; asprou.markos@ucy.ac.cy; elias@ucy.ac.cy).

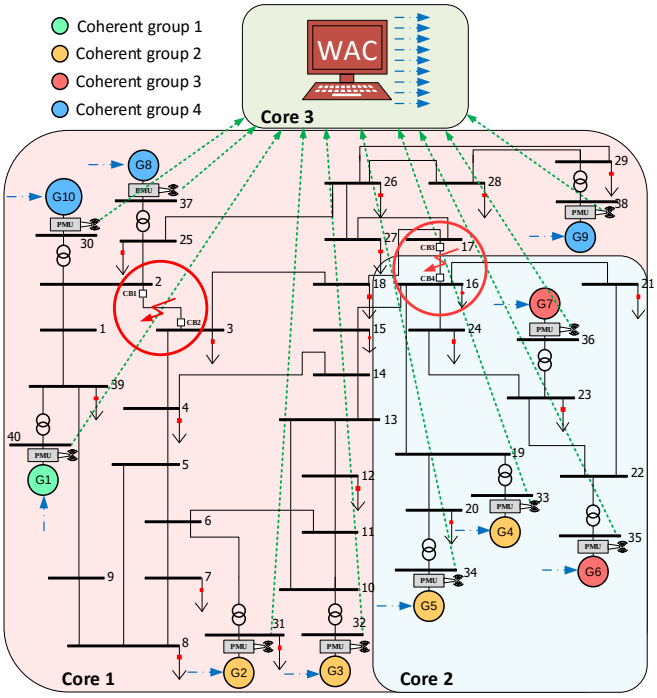

Fig. 1. IEEE 39-bus test system illustrating: (i) the examined disturbances, (ii) the separation of the system into 3 cores for *real-time* simulation, and (iii) the coherent generators (each generator color implies a different coherent group).

similar approach for coordinating simultaneously through a wide area controller all the synchronous generators and the renewables in order to increase the overall damping capability of the system, is shown in [9], [10] and [11].

Considering the coordination of synchronous generators, it is beneficial to coordinate the excitation systems by deriving a supplementary WAC signal, in addition to the one provided by the PSS, having as a goal to increase the small-signal stability [11], [12]. More specifically, in [5] and [13] the authors have shown the significant improvement on the system's damping capability when the wide area controller is included in addition to the PSS devices. The simultaneous coordination of the synchronous generators and DFIG wind turbines was presented in [10], by utilizing the PSSs of three generators and the Power Oscillation Dampers of three renewable sources respectively. Finally, in [14] PSS-based controllers are presented for regulating renewable plants which, among other capabilities, can receive wide area control signals in order to contribute to the system's small signal stability.

The majority of the published WAC methodologies propose the coordination of the exciter only (directly or indirectly, through the PSS). This is mainly due to the faster response of the excitation system compared to the governor and the availability of the PSSs output signal on the input of the former (e.g. [4], [10], [11]). However, the coordination of the governor can be proven to be beneficial for the damping of local and especially inter-area oscillations, since it is directly related to the control of the generators' frequency.

Furthermore, it is a common practice to regulate the coordination signals provided by the wide area controller (e.g., [4], [15], [16]) in order to avoid high control efforts and high contribution levels. Generally, this is accomplished by adding a constant gain at the output of the WAC. This regulation constant is tuned by the designer, based on the system's behavior and it can be far from the optimal since its value should change according to the contingency's nature. A similar approach is followed for the tuning of the Automatic Generation Control (AGC), where the constant control gains are determined either through case study simulations or by trial-and-error [17]. However, in contrast to the WAC case, methodologies have been proposed for the online tuning of the AGC. More specifically, in [17] a dynamic tuning of the control gains is presented, which also considers the effect of the wind farms' penetration in the system. In [18], an adaptive AGC is proposed with self-tuning gain capabilities in order to avoid the over-regulation caused by the system operators.

This paper presents novel methodologies for obtaining WAC signals suitable for the coordination of the governors and PSSs. More specifically, the first contribution of this work is the development of a methodology which can be used either for coordinating all the governors of the system (in case the system does not utilize PSSs) or for coordinating simultaneously both the governor and PSS of each generator through a common WAC signal, without any modification of the signal formulation. Note that for the exciter coordination, a conventional signal (based on [15]) is considered, where slight modifications are made. The second contribution of this paper is the development of a methodology for adaptive tuning. The aim here is to obtain weights intended for the regulation of the WAC signals. Electro-Magnetic Transient (EMT) simulations are performed on the IEEE 39-bus dynamic test system in order to investigate the improvement of the wide area controller's performance when the new coordination signals and the adaptive tuning method are applied. For this reason, offline and *real-time* (through OPAL-RT equipment) simulations are performed. Fig. 1 shows the IEEE 39-bus dynamic test system, as well as its separation into cores for the *real-time* simulation (Section V). It is worth mentioning that dynamic load models are included for more realistic simulations. The evaluation of the proposed WAC performance is accomplished by utilizing the Prony analysis tool. Furthermore, the coherency concept is required in this work in order to reduce the number of PMUs needed by the proposed scheme. Finally, both measurement errors and data delays/dropouts, as described in [19], have been considered for the testing of the proposed scheme. As indicated in [19], the data delays (which impact more the WAC performance) can be overcome successfully through the use of a linear predictor. In this sense, data delays are out of the scope of this paper.

In summary, the main contributions of this paper are: 1) the development of a new methodology for the coordination of the governors, 2) the simultaneous coordination of both the governor and the PSS through a single WAC signal, 3) the development of an adaptive self-tuning algorithm for the on-line regulation of the WAC contribution level, 4) the reduction of the required synchronized measurements through coherency, and 5) the validation of the proposed scheme through *real-time* simulations. The contributions of this work improve considerably the WAC performance under various contingencies, in the presence of dynamic loads as well as

realistic measurement errors.

II. Conventional Wide Area Control Design

This section discusses the procedure for the development of a conventional wide area controller, which is shown in detail in [15]. This is necessary for providing the basis for the next section where the development of the proposed method is presented. Note that the conventional WAC of this section will be used for comparison later on, to evaluate the effectiveness of the proposed scheme.

A. Wide Area Measurements

The successful formulation and operation of a wide area controller depends highly on the availability of synchronized measurements from the system. Therefore, in this study PMUs are assumed to be installed at all the generator buses, as shown in Fig. 1. This is due to the fact that the methodology requires the terminal voltages (v_t), the frequencies (f), and the rotor angles (δ) from all the generators. The voltages and frequencies can be obtained directly by the PMUs. In [15] the rotor angle is assumed to be available as well, but in reality, the majority of the commercial PMUs cannot provide it. For this reason, the rotor angle is calculated using synchronized voltage and current measurements, according to [19]. Therefore, by expressing all the generator vectors into the *d-q* frame and by considering only the *d*-axis, the rotor angle (relative to the terminal voltage of the generator) can be calculated as follows:

$$\delta = \arctan\left(\frac{x_q i \cos(\varphi)}{v_t + x_q i \sin(\varphi)}\right) \tag{1}$$

where i is the terminal generator current, φ represents the phase angle difference between the voltage and current measurements, and x_q stands for the q-axis synchronous reactance of the generator. It is to be noted here that by considering that the generator's synchronous reactances are known, the rotor angle can be estimated solely from PMU measurements.

B. Necessary Models for Wide Area Control Development

The objective of the methodology in [15] is to make all the necessary steps to obtain a new state space representation of the system, suitable for deriving the WAC signals. This is achieved by reformulating the system into a closed form and applying a change of variables. The latter is done in order to have as new state variables the generators' terminal voltages, expressed on the *d-q* axis (v_d and v_q). To apply the methodology, models of the generator and the power system are required.

For the modelling of the synchronous generator, the fourth order model and the stator dynamic equations are required [20], [21]. The fourth order model (shown in (2)-(4)) is considered here, since it was found adequate for control design in [22]. Equations (2) and (3) describe the relationship between the stator currents (i_d and i_q), the internal (e_d and e_q) and field (e_{fd}) voltages, while (4) represents the swing equation [23]. However, looking at (2)-(3) one can note that they do not include the terminal voltage of the generator, which is going to be the system's state. For this reason, the stator dynamic equations are also considered in (5)-(6), to connect the terminal voltage with the internal voltage and stator current.

$$T'_{dok}\dot{e}'_{qk} = -e'_{qk} - (x_{dk} - x'_{dk})i_{dk} + e_{fdk} \tag{2}$$

$$T'_{qok}\dot{e}'_{dk} = -e'_{dk} + (x_{qk} - x'_{qk})i_{qk} \tag{3}$$

$$\frac{2H_k\omega_{puk}}{\omega_s}\frac{d\omega_k}{dt} + \frac{D_k\omega_{puk}}{\omega_s}\frac{d\delta_k}{dt} = P_{mk} - (v_{dk}i_{dk} + v_{qk}i_{qk}) \tag{4}$$

$$v_{dk} = e'_{dk} - r_{sk}i_{dk} + x'_{qk}i_{qk} \tag{5}$$

$$v_{qk} = e'_{qk} - r_{sk}i_{qk} - x'_{dk}i_{dk} \tag{6}$$

where T'_{do} and T'_{qo} stand for the open circuit time constants (in seconds). x_d and x_q are the synchronous reactances of the generator k, while x'_d and x'_q are its transient reactances (in p.u.). P_m represents the mechanical power, ω is the rotor speed, while ω_s is the synchronous speed. H, D, and r_s represent the generator's inertia constant, damping coefficient, and stator resistance respectively (all in p.u.). Lastly, δ stands for the rotor angle (in radians).

The power network can be described by the following two current equations. The first one represents the generator buses, while the second one refers to all the remaining buses. G' and B' stand for the real and imaginary elements of the admittance matrix:

$$\frac{-1}{jx'_{dk}}(e'_{dk} + (x'_{qk} - x'_{dk})i_{qk} + je'_{qk})e^{j(\delta_k - \pi/2)} + \sum_{j=1}^{m}(G'_{kj} + jB'_{kj})v_j e^{j\theta_j} = 0 \tag{7}$$

$$\sum_{j=1}^{m}(G'_{kj} + jB'_{kj})v_j e^{j\theta_j} = 0 \tag{8}$$

C. Conventional Wide Area Control Formulation

The overall objective of the WAC is to estimate the appropriate coordination signals intended for the generator's local controllers. Therefore, it is important to identify the local controllers and their respective local signals to be coordinated. In this study, the generators are implemented to consider the exciter DC2A and the general-purpose governor according to [24]. Consequently, the local control signals that the wide area controller will interact with are the excitation signal (e_{fd}) and the steam valve output (P_{GV}). Looking at (2)-(6) one can note the excitation signal, but not the steam valve output. Therefore, the following turbine model is required in addition to (2)-(6), since it connects the governor's P_{GV} with the generator's P_m:

$$P_m = \frac{1}{1 + sT_{CH}}\frac{1 + sT_{RH}F_{HP}}{1 + sT_{RH}}P_{GV} \tag{9}$$

where T_{CH} represents the delay due to the steam chest/inlet piping, T_{RH} stands for the delay of the re-heaters and F_{HP} is the total turbine power developed in the high-pressure cylinder. The delays are expressed in seconds and the power in per unit.

As it is aforementioned, for the formulation of the WAC signals, a new state space representation of the system is required. These new dynamic equations will have as state variables the generators' terminal voltages. The procedure to derive these expressions can be summarized into the following three steps:

1) The non-generator bus voltages are expressed in terms of the generators' terminal voltages, based on (7) and (8).

2) The expressions of the generators' internal voltage and stator current are derived in terms of their terminal voltage, according to (5), (6) and (7).
3) The resulted expressions are substituted in (2)-(4).

Following the previous steps, the new dynamic equations of the power system are:

$$\dot{v}_{dk} = a_{1k} v_{dk} + a_{2k} v_{qk} + p_{1k} e_{fdk} + \psi_{dk} \quad (10)$$

$$\dot{v}_{qk} = b_{1k} v_{dk} + b_{2k} v_{qk} + p_{2k} e_{fdk} + \psi_{qk} \quad (11)$$

$$\frac{2H_k}{\omega_s}\frac{d\omega_{puk}}{dt} + \frac{D_k}{\omega_s}\frac{d\omega_{puk}}{dt} = P_{mk} - G_{kk}^{\ f}(v_{dk}^2 + v_{qk}^2) - \psi_{\omega k} \quad (12)$$

where a_1, a_2, b_1, b_2, p_1, p_2 are parameters which mainly depend on the network topology (admittance matrix) and the parameters of the generator (reactances and time constants). ψ_d, ψ_q, and ψ_ω are the inter-generator interactions (or coupling perturbation terms) from other generators on the k^{th} generator. More details regarding the methodology and the expressions of all these terms are provided in [15].

The new state space representation of the system can be used now to obtain the WAC signals. To achieve this, firstly the terminal voltages and rotor speeds are substituted by their error compared to their steady state values (dv_d, dv_q and $d\omega$). The reason for applying this change is actually to nullify the contribution of the wide area controller when the system is in steady state.

The next step is to find in the resulting equations the inputs of the local controllers (namely the excitation signal e_{fd} and the steam valve output P_{GV}). In the case where a local control input is not directly available (e.g., absence of P_{GV} in (12)), then an input-output linearization is applied [15]. Then each control input is decomposed into a local and a global part, with the latter selected to cancel out all the perturbation terms of the equations (ψ_d, ψ_q, and ψ_ω). Hence, the following expressions present the derived WAC signals intended for the coordination of the exciter and the governor:

$$e_{fdk}^{g} = \gamma_k \frac{-(\psi_{dv_d}^k dv_{dk} + \psi_{dv_q}^k dv_{qk})}{p_{1k} dv_{dk} + p_{2k} dv_{qk}} \quad (13)$$

$$p_{GVk}^{g} = -\gamma_k \frac{T_{CHk}\dot{\psi}_{\omega}^k}{F_{HPk}} \quad (14)$$

As it is pointed out in [15], γ_k is a constant parameter which serves as a weighting factor in order to regulate the contribution level of the WAC. This regulation gain is required in order to avoid instability of the power system. This is because a simplified model of the synchronous machine is considered (fourth order) for the derivation of the wide area control signals, while the local controllers' limitations are not taken into account. It is worth mentioning that this parameter is tuned by the designer according to the system and the contingency. A general practice is to utilize a small weighting value (in this study γ_k=0.2 for the conventional WAC) in order to ensure the damping of the majority of the contingencies which can take place in the power system. However, this practice has as a result to restrict the WAC damping capability and to reduce its performance.

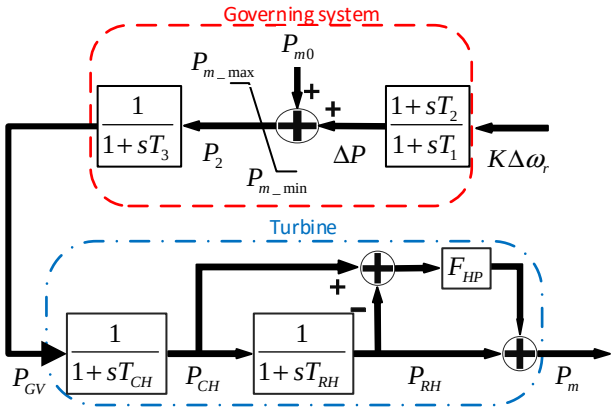

Fig. 2. Steam and governing system configuration of general-purpose governor.

III. Proposed Governor and PSS Wide Area Control

The methodology in [15] coordinates the excitation signal and the steam valve output, bypassing in that way the operation of the PSS in the case that they exist in the generator system. Therefore, in this section, a methodology is developed which aims to coordinate effectively all the local controllers of the generator for increasing the small-signal stability of the system. Note that the proposed scheme is flexible to be applied to systems with or without PSSs. More specifically, the objective here is to derive coordination signals, which can increase the damping of local and especially inter-area oscillations by coordinating effectively all the governors and PSSs of the system. It is worth mentioning that for the exciter coordination, a conventional WAC signal will be considered (shown in (13)).

A. Development of governor coordination signals

For the formulation of the proposed governor WAC, the following model of the multi-machine power system dynamics is considered instead of the swing equation shown in (4),

$$J_k \frac{d^2\delta_k}{dt^2} = P_{mk} - e_k^{'2} G_{kk}^r - \sum_{\substack{j=1 \\ j\neq k}}^{n} (C_{kj}\sin(\delta_{kj}) + D_{kj}\cos(\delta_{kj})) \quad (15)$$

where

$$\delta_{kj} = \delta_k - \delta_j\ ,\ C_{kj} = e_k^{'} e_j^{'} B_{kj}^r\ ,\ D_{kj} = e_k^{'} e_j^{'} G_{kj}^r$$

This set of equations is usually utilized for constructing Lyapunov functions intended for the transient stability assessment and to derive equations which describe the mutual motion of paired machines [23]. The important advantage of utilizing this equation instead of (4), is that there is no need to go into the three-step procedure of [15], presented previously. The reason is that (15) is already in a suitable form where the local terms are separated completely from the inter-generator interactions (superposition term).

Equation (15) depends directly on the self- and transfer-admittances of the reduced network (G^r and B^r). The problem that arises is that the reduction of the admittance matrix down to the generator buses either assumes static and linear loads or it completely neglects them [23]. To overcome this issue and utilize a more suitable expression for the reduced admittance matrix, the reformulation derived from the expression of the non-generator bus voltages in terms of the generators' terminal voltages is considered (step 1 of Section II). More specifically,

in this step the admittance matrix is reformulated (into a closed form) to consider only the generator buses through the current equations of (7) and (8).

By considering (15), the formulation of the governor coordination signals can be illustrated. As it is aforementioned in Section II.C, the variables of the equation must be substituted by their difference compared to their steady state values (*de* and *dω*). Due to the fact that the internal voltage of each generator cannot be measured directly by the PMUs, (5) and (6) are utilized for estimating e'_d and e'_q, respectively. The result is then substituted in (15) through the following expression:

$$de'^2_k = de'^2_{dk} + de'^2_{qk} \tag{16}$$

One of the main novelties of this work is that the derived WAC will not interact with the local control signal P_{GV} (like in the case of [15]), but instead it will coordinate the governing system through its input signal (rotor speed deviation $\Delta\omega_r$). For this reason, the equations of the turbine and the governor system are required. These can be derived from (9) and Fig. 2. More specifically, the turbine equations are the following:

$$P_{mk} = (P_{CHk} - P_{RHk})F_{HPk} + P_{RHk} \tag{17}$$

$$T_{CHk}\dot{P}_{CHk} = P_{GVk} - P_{CHk} \tag{18}$$

$$T_{RHk}\dot{P}_{RHk} = P_{CHk} - P_{RHk} \tag{19}$$

where P_{CH} and P_{RH} represent the steam pressure and the re-heated steam pressure in per unit, respectively.

The derived equations describing the governor operation are:

$$T_{3k}\dot{P}_{GVk} = P_{2k} - P_{GVk} \tag{20}$$

$$P_{2k} = P_{m0k} + \Delta P_k \tag{21}$$

$$T_{1k}\Delta\dot{P}_k = -K(\Delta\omega_{rk} - T_{2k}\Delta\dot{\omega}_{rk}) - \Delta P \tag{22}$$

where T_1, T_2 and T_3 are time constants (in seconds), while K is the speed regulation constant.

In order to develop the appropriate coordination signals, which will interact with the input of the governor, the input-output linearization approach has been adopted. This is a methodology which actually results to the implementation of non-linear decoupling control signals. The idea behind this technique is to differentiate the equation where the end-up variable to be controlled indirectly exists (e.g., (15) for the case of P_m), until the desirable input appears ($\Delta\omega_r$). The following expression presents the result of applying the input-output method on (15), until $\Delta\omega_r$ shows up:

$$\frac{d^4\omega_k}{dt^4} = \frac{1}{J_k}\left[F_{HPk}\left[\begin{array}{c}-K\dfrac{((\Delta\omega^l_{rk}+\Delta\omega^g_{rk})-T_{2k}\Delta\dot{\omega}_{rk}}{T_{1k}T_{3k}T_{CHk}} \\ -\dfrac{\Delta P_k}{T_{1k}T_{3k}T_{CHk}}-\dfrac{\ddot{P}_{CHk}}{T_{CHk}}\end{array}\right] + \ddot{P}_{RHk}(1-F_{HPk}) - \ddot{e}'^2_k G^g_{kk} + \dddot{\psi}_{gk}\right] \tag{23}$$

where

$$\psi_{gk} = \sum_{\substack{j=1\\ j\neq k}}^{n}(de'_k de'_j B^g_{kj}\sin(\delta_{kj}) + de'_k de'_j G^g_{kj}\cos(\delta_{kj})) \tag{24}$$

G^g and B^g represent the reformulated admittance matrix. Note that to derive the expression of (23), (17)-(22) are utilized.

To obtain the suitable WAC signal, the input to be controlled is decomposed into a local ($\Delta\omega_r^l$) and a global part ($\Delta\omega_r^g$). The latter term represents the interaction of the wide area controller with the local controller and it is determined by selecting the global signal to cancel out the inter-generator interactions (ψ_g). This results in deriving a novel WAC signal intended for the coordination of the governor, through its input signal:

$$\Delta\omega^g_{rk} = -\gamma_k\frac{T_{1k}T_{3k}T_{CHk}\ddot{\psi}_{gk}}{KF_{HPk}} \tag{25}$$

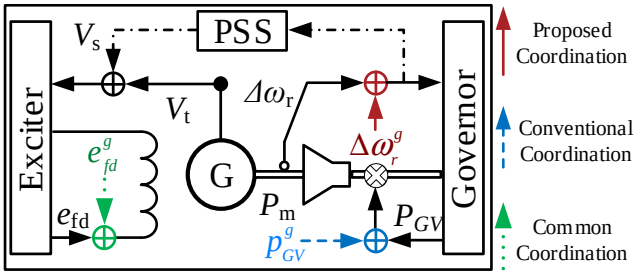

Fig. 3. Illustration of the proposed and conventional coordination signals. Green dotted line represents the common signal, which remains the same for both schemes. Dash-dotted line indicates the case where PSS is optionally installed.

B. Simulation specifications and evaluation

In order to evaluate the damping capability of the proposed WAC (PropWAC) and furthermore to illustrate its enhanced performance, the proposed scheme is compared to a conventional wide area controller (in this case the one presented in [15], hereafter referred to as ConvWAC). It is important to mention here that for the exciter coordination, the proposed scheme considers the same WAC signal as the conventional method as it is shown in Fig. 3. The aim is to illustrate clearly the performance enhancement when the WAC signal of (25) is utilized for the coordination of the governor instead of the conventional one of (14). Both methodologies are implemented and tested in the IEEE 39-bus dynamic test system, where coordination is applied on the exciter DC2A and the general-purpose governor of all the generators. Note that as a benchmark, the scenario where no WAC (NoWAC) exists in the system is considered. The test system and WAC are constructed using EMT offline simulations on MathWorks Simulink.

It is also worth mentioning that conversely to the conventional WAC of [15], a rate limiter is applied on all the coordination signals of the exciter and the governor. The reason behind this addition is to avoid the wearing-and-tearing of the local controllers due to the abrupt changes (resulting from the application of the WAC signals) and thus to allow the smoother transition from the one state to the other. This is especially the case for the governor, which has a slower response compared to the exciter operation. Therefore, two different rate limits (faster/slower) are utilized on the WAC signals intended for coordinating the exciter and the governor.

Furthermore, for more realistic simulated conditions, non-linear load models are included in the simulations of this work instead of the commonly used, ideal constant-power loads. The behavior of the dynamic loads changes significantly in transient conditions compared to their steady state behavior. It should be noted that the ConvWAC performance is sensitive to the presence of dynamic loads [9]. The exponential dynamic load model is considered here which is a time-variant, voltage-

depended load described using the following equations [25]:

$$P(s)=P_0\left(\frac{V}{V_0}\right)^{n_p}\frac{1}{1+T_p s} \quad (26)$$

$$Q(s)=Q_0\left(\frac{V}{V_0}\right)^{n_q}\frac{1}{1+T_q s} \quad (27)$$

where V, P and Q stand for the positive sequence voltage, the active power and the reactive power of the load respectively. Note also that V_0, P_0 and Q_0 are the initial values of these quantities. Furthermore, T_p and T_q are the recovery time constants for the active and reactive power, respectively. Finally, n_p is the active while n_q is the reactive exponent, which control the nature of the load. The parameter values of all the exponential dynamic models considered in this work, are based on the parameter estimation shown in [26]. Therefore, [n_p n_q]=[0.3425 2.4951] and [T_p T_q]=[131.78 124.11] in order to obtain an intense dynamic behavior during transient conditions.

The successful operation of a wide area controller includes the complete compensation of all the local and inter-area oscillations. For this reason, the terminal voltage of the generators is utilized to illustrate the local oscillations, while the speed difference of two distant generators is considered to present the inter-area oscillations. In order to provide more analytical results regarding the damping performance of the proposed and the conventional coordination schemes, the Prony analysis is also used. This is a widely known, measurement-based method suitable for ringdown analysis and small-signal properties' estimation of a damped signal [3]. Prony analysis is extensively used in the studies of well-established organizations, such as in the recent reports of ENTSO-E [27]. More specifically, this analysis tool can extract the damping ratio (ζ) and frequency (f) of the dominant local and inter-area modes from the measurements. These are estimated through their energy content [28] and their constant appearance irrespective to the order of the Prony model [29]. Note that the higher the damping ratio the better the WAC performance is.

C. Case study 1: Performance of the proposed methodology

All the examined scenarios (NoWAC, ConvWAC and PropWAC) are tested considering a 5-cycle three-phase fault on the line connecting bus 2 to bus 3 at t= 1s, followed by the line tripping at t= 1.1s and its reclosing at t= 1.7s (Fig. 1). Note also that the static loads of buses 4, 8, 15, 21 and 27 are substituted by their respective exponential dynamic loads. Furthermore, it is important to mention here that the weighting factor (γ_i) of all the WAC signals is tuned by trial and error. Therefore, it is found that for the ConvWAC scheme γ_i=0.2 is applied on both WAC signals of (13) and (14), for all the generators of the system. In the case of the proposed scheme, γ_i=0.1 is utilized for the exciter coordination of (13), while γ_i=0.3 is considered for the governor coordination of (25). For the graphical illustration of the simulation results, the terminal voltage of generator 2 (v_2) and the speed difference between generators 7 and 10 are considered (w_7-w_{10}). Figures 4a and 4d show that the proposed coordination outperforms the ConvWAC and NoWAC scenarios in damping both local and inter-area oscillations. More specifically, due to the presence of non-linear loads, the ConvWAC scenario has the worst performance (even compared to the NoWAC scenario), especially in the case of inter-area oscillations where a small oscillation remains undamped. This outcome can be further verified through the Prony analysis results of Table I. Here, the increased damping ratio in the case of both local and inter-area modes indicates the improvement of the WAC performance when the proposed governor coordination is considered.

D. Case Study 2: Coordination of governor and PSS

The significant advantage of coordinating a local controller through its input signal is that it provides the flexibility and capability of coordinating simultaneously other local controllers, which might use the same input. This is actually the case of the governor and the PSS, which both have as input the rotor speed deviation ($\Delta\omega_r$). Therefore, as shown in Fig. 3 the same WAC signal of (25) can be used for the simultaneous coordination of both governor and PSS, in the case where PSSs exist in the system (dash-dotted line).

The coordination of the PSS (in addition to the governor) will damp faster and more effectively the inter-generator interactions. This is achieved by coordinating (through PSS) the electric torque component that is generated due to the exciter's output. The idea of utilizing simultaneously the governor and PSS to damp the perturbation terms (ψ_g) is based on the utilization of both the mechanical (governor) and the electrical (PSS) part of the generator for increasing the system's small-signal stability.

For evaluating the performance of the proposed scheme in the presence of PSS, the latter is added into all the generators of the system according to [24]. In this case study, a 5-cycle three-phase fault is applied on the line connecting bus 16 to bus 17, at t= 1s. Once again, the line trips for 0.6 s in order to clear the fault and then it recloses. Furthermore, exponential dynamic load models are considered to exist on buses 4, 15, 25, 27 and 29. Note that the same weighting factors as in the previous subsection are applied here as well. Figs. 4b and 4e along with Table I present the graphical and numerical results of the simulation. For the graphical illustrations of the local and inter-area signals, the terminal voltage v_{10} and the speed difference w_2-w_7 are considered respectively. The simulation results of this case study illustrate that the PropWAC scheme has the best performance over the other two schemes since it achieves an effective damping of local and inter-area modes. It is also worth mentioning that from Fig. 4b it can be derived that the ConvWAC scenario fails to compensate promptly the local oscillation. The Prony analysis results of Table I present clearly that the proposed scheme provides significant additional damping of the local and inter-area modes compared to the NoWAC and ConvWAC schemes.

IV. Adaptive Tuning of WAC Signals

Based on the formulation of the proposed and conventional wide area controllers, one can argue that their performance depends highly on one crucial parameter, the weighting factor γ_i. This statement is generally true, since an incorrect tuning of the WAC contribution to the generators' local controllers, can lead the system to instability. Therefore, as it is clearly pointed out in [15], the main issue of the methodology presented at the end of Section II.C, is that the contribution level of the WAC

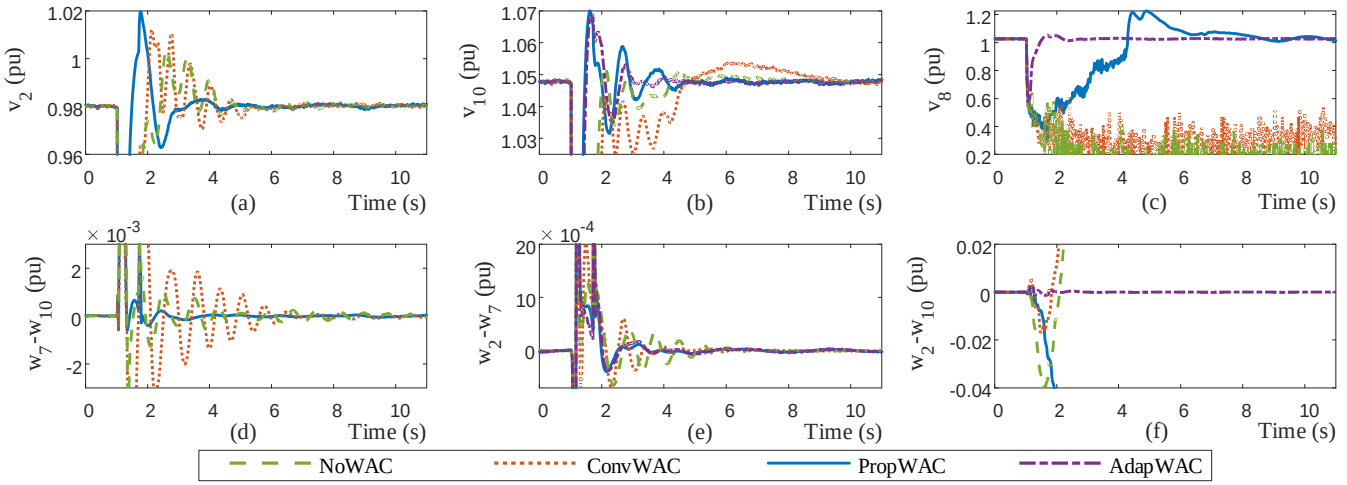

Fig. 4. Illustration of the performance of the NoWAC, ConvWAC, PropWAC and AdapWAC in compensating the local ((a)-(c)) and inter-area ((d)-(f)) modes for all the case studies: (i) Case Study 1: (a) and (d), (ii) Case Study 2: (b) and (e), (iii) Case Study 3: (c) and (f)

TABLE I
PRONY ANALYSIS RESULTS FOR ALL THE EXAMINED CASE STUDIES

Case Study No.		NoWAC		ConvWAC		PropWAC		AdapWAC	
1	**Type**	ζ(%)	*f*(Hz)	ζ(%)	*f*(Hz)	ζ(%)	*f*(Hz)		
	Local mode	8.42	1.6	6.65	1.6	13.7	1.5		
	Inter-area mode	21.1	0.81	14.3	0.77	31.7	0.81		
2	**Type**	ζ(%)	*f*(Hz)	ζ(%)	*f*(Hz)	ζ(%)	*f*(Hz)	ζ(%)	*f*(Hz)
	Local mode	15.7	1.4	11.9	1.6	17.6	1.6	23.7	1.5
	Inter-area mode	17.5	0.74	18.3	0.76	30.7	0.69	28.8	0.74
3	**Type**	ζ(%)	*f*(Hz)	ζ(%)	*f*(Hz)	ζ(%)	*f*(Hz)	ζ(%)	*f*(Hz)
	Local mode	Instability		Instability		6.14	1.5	14.8	1.6
	Inter-area mode	Instability		Instability		Instability		27.3	0.73

signals must be tuned a priori manually by the designer. However, the weighting factor cannot remain constant at all times, since its value must change according to the nature and the location of the contingency.

In this work a method to tune adaptively the weighting factor of the coordination signals is developed. The overall idea is that the contribution of the coordination signals should take into account the connectivity of the power system in order to identify the strongly connected areas. The information about the connectivity is especially needed for compensating the inter-area oscillations, since the latter results from the existence of weak tie lines in the grid. A straightforward way to estimate the electric connectivity between generators is as follows ([23]),

$$w_{kj} = e_k^{'} e_j^{'} Y_{kj}^{\ g} \tag{28}$$

where Y^g represents the magnitude of the reformulated admittance matrix, which is also known as the electric distance in a power system. It is worth mentioning here that the reformulated admittance matrix is utilized in (28), instead of the reduced admittance matrix. Note that the electric connectivity depends indirectly (through the internal voltages) on the generators' terminal voltages. Like in the case of Section III.A, the internal voltages are estimated through synchronized voltage and current measurements based on the stator dynamic equations shown in (5) and (6).

As shown in (28), to apply correctly the concept of electric connectivity as a weighting factor on the coordination signals (intended for the exciter, governor and PSS) it is essential to consider that electric connectivity does not depend on the k^{th} generator and the rest of the generators as a whole, but on each generator pair *k*-*j* separately. Therefore, the weighting scheme derived from (28) will have the ability to regulate exclusively each inter-generator interaction between generators *k* and *j*, according to their electric connectivity. To better illustrate this, the proposed governor/PSS coordination of (25) will become:

$$\Delta\omega_{rk}^{g} = -\frac{T_{1k}T_{3k}T_{CHk}}{KF_{HPk}}\frac{d^3}{dt^3}\left[\sum_{\substack{j=1\\ j\neq k}}^{n}\left(\frac{1}{w_{kj}}\left(\begin{matrix} de_k^{'}de_j^{'}B_{kj}^{g}\sin(\delta_{kj}) \\ +de_k^{'}de_j^{'}G_{kj}^{g}\cos(\delta_{kj})\end{matrix}\right)\right)\right] \tag{29}$$

The superposition term of (29) is derived by substituting (24) into (25), which is necessary for illustrating clearly the regulation of each inter-generator interaction between generators *k* and *j*. Note that in a similar way, the weighting scheme is applied also into the perturbation terms of the exciter WAC in (13). The reason for utilizing the inverse of the electric connectivity as the weight of the inter-generator interactions is because it is desirable to apply high WAC contribution on sets of generators which are connected through weak tie lines and the opposite where strongly connected generators exist. The important advantage here is that the contribution of the WAC signals will be tuned on-line and adaptively according to the PMU measurements obtained from the generators.

To illustrate the impact of considering the adaptive tuning concept on the WAC architecture, the results of Case Study 2 include also the system's response when the proposed adaptive method is applied on the coordination signals of the PropWAC scenario ((13) and (25)). Based on Figs. 4b and 4e, one can note that the resulted adaptive WAC (AdapWAC) scenario provides slightly better damping of the local oscillations, while it has almost the same performance in compensating the inter-area modes compared to the PropWAC scenario. The numerical

results of Table I further validate the performance of the AdapWAC scenario in successfully damping all the modes.

A. Case Study 3: Adaptive tuning under high penetration of non-linear loads

In order to illustrate clearly the actual contribution of the AdapWAC scenario, a slightly different case study is also included in this section. More specifically, the same disturbance and fault-clearing on the line connecting bus 16 to bus 17 is considered, but more non-linear loads are assumed in this case study. Note that dynamic loads are placed on buses 4, 8, 15, 21, 23, 25, 27, 29 and that the same weighting factors and simulation specifications (as previously discussed) are utilized here (PSSs are considered into all the generators). The derived results are presented in Figs. 4c and 4f, where the terminal voltage v_8 and the speed deviation w_2-w_{10} are used for viewing the local and inter-area oscillations, respectively. As it is illustrated, only the AdapWAC scheme is capable of damping effectively all the dominant modes and preserving the system's stability, outperforming the other schemes. This outcome illustrates that it is essential to incorporate an adaptive-tuning procedure into the WAC scheme, in order to ensure the continuous stability of the system. These conclusions can be further verified through the Prony analysis results of Table I, where it is evident that the application of the proposed adaptive-tuning on the proposed WAC has increased its damping performance, while all the other scenarios fail to keep the system stable.

V. Real-Time Simulation

Although the offline simulation results of Fig. 4 and Table I have illustrated clearly the performances of the proposed coordination and the adaptive tuning methodologies, their actual evaluation can only be ensured through real-time simulation. For this reason, an OPAL-RT *real-time* simulator has been utilized to obtain in *real-time*, more accurate simulations for further validation. More specifically, three cores of the OP5700, each one equipped with an Intel Xeon E5 8 Core CPU at 3.2 GHz and with 8 GB RAM, were considered here. Two cores were used for implementing the *real-time* model of

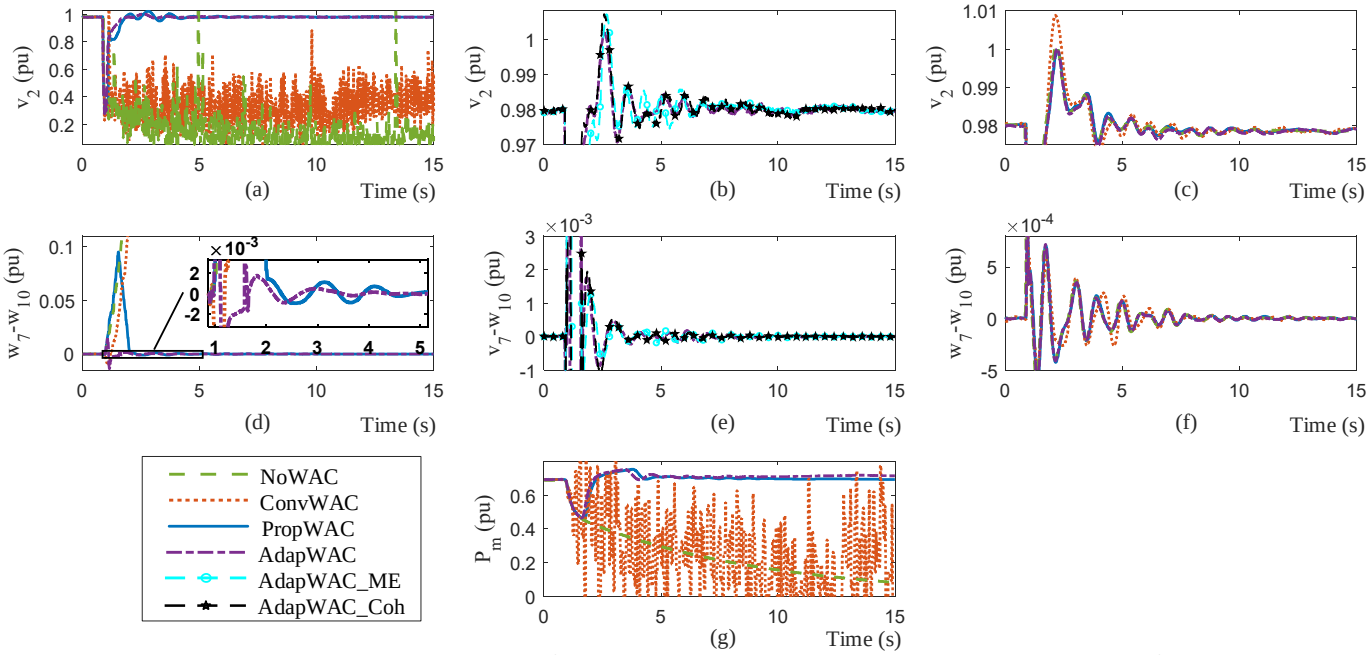

Fig. 5. Real-time simulation results illustrating: (i) comparison of NoWAC, ConvWAC, PropWAC and AdapWAC during three-phase fault in compensating the local (a) and inter-area modes (d), (ii) comparison of AdapWAC, AdapWAC_ME and AdapWAC_Coh during three-phase fault in compensating the local (b) and inter-area modes (e), (iii) comparison of NoWAC, ConvWAC, PropWAC and AdapWAC during G1 trip in compensating the local (c) and inter-area modes (f) and (iv) comparison of the governor output (g) for the NoWAC, ConvWAC, PropWAC and AdapWAC scenarios.

TABLE II
PRONY ANALYSIS RESULTS OF THE REAL-TIME SIMULATION FOR ALL THE EXAMINED CASE STUDIES

Case Study No.	1							
Scenario	**NoWAC**		**ConvWAC**		**PropWAC**		**AdapWAC**	
Type	ζ(%)	*f*(Hz)	ζ(%)	*f*(Hz)	ζ(%)	*f*(Hz)	ζ(%)	*f*(Hz)
Local mode	Instability		Instability		9.68	1.8	12.28	1.8
Inter-area mode	Instability		Instability		18.2	0.8	31.5	0.72
Case Study No.	2				3			
Scenario	**AdapWAC**		**AdapWAC_ME**		**AdapWAC**		**AdapWAC_Coh**	
Type	ζ(%)	*f*(Hz)	ζ(%)	*f*(Hz)	ζ(%)	*f*(Hz)	ζ(%)	*f*(Hz)
Local mode	12.28	1.8	12.28	1.8	12.28	1.8	11.65	1.9
Inter-area mode	31.5	0.72	26	0.77	31.5	0.72	26.9	0.74
Case Study No.	4							
Scenario	**NoWAC**		**ConvWAC**		**PropWAC**		**AdapWAC**	
Type	ζ(%)	*f*(Hz)	ζ(%)	*f*(Hz)	ζ(%)	*f*(Hz)	ζ(%)	*f*(Hz)
Local mode	7.72	1.5	7.14	1.8	8.19	1.8	8.34	1.9
Inter-area mode	14.2	0.69	13.2	0.8	15	0.65	15.7	0.7

the IEEE 39-bus test system, while one core was required for running the WAC algorithms as shown in Fig. 1. Apart from the evaluation of the proposed methods in *real-time*, this section also examines the sensitivity of the adaptive tuning methodology in the presence of measurement errors. In addition, the reduction of the required synchronized measurements through the coherency concept is also investigated.

A. Case Study 1: Real-time simulation results for three-phase fault

The disturbance considered into the *real-time* simulation is the same one as the one presented in Section III.C. In this case study, dynamic loads were placed on buses 8, 15, 21, 23, 25, 27 and 29. Once again, the aim is to compare the performances of all the examined scenarios (NoWAC, ConvWAC, PropWAC and AdapWAC) in *real-time*, using graphical (Figs. 5a and 5d) and numerical results (Table II). More specifically, Fig. 5a presents the terminal voltage v_2, while Fig. 5d the speed deviation w_7-w_{10}. The results show clearly that the NoWAC and ConvWAC scenarios fail to keep the system stable at the event of the fault, leading it to instability. Therefore, only the PropWAC and AdapWAC scenarios are capable in this case of damping effectively all the local and inter-area oscillations. For the effective comparison between the two scenarios, the Prony analysis results are utilized. According to Table II, one can note that the AdapWAC has better performance compared to the PropWAC scenario in damping effectively all the oscillations. The enhanced performance of the governor in the cases of the PropWAC and AdapWAC can be also evaluated through Fig. 5g, which illustrates the output signal (P_m) of the governor of generator 2 during the fault, for each scenario.

B. Case Study 2: Impact of measurement errors on adaptive tuning

Based on (28) and (29), it is obvious that the proposed method is heavily depended on synchronized measurements. Therefore, in order to consider realistic conditions into the *real-time* simulation, the proposed scheme is tested under the presence of realistic measurement errors. To achieve this, the procedure presented in [19] is adopted here. More specifically, in [19] the authors have applied realistic measurement errors to identify the impact of measurement quality and accuracy on the ConvWAC performance. The examination included the measurement errors deriving from both instrument transformers and PMUs. In addition, the PMU measurement errors considered in the study were changing during dynamic conditions from their steady state values to their dynamic ones, according to the dynamic compliance requirements of [30]. The adopted measurement errors considered here are illustrated in Table III. More details considering the measurement errors and their utilization can be found in [19]. The outcome when the measurement errors are applied to the AdapWAC (AdapWAC_ME scenario) is presented in Figs. 5b and 5e. As shown, the presence of measurement errors has a small effect on the performance of the AdapWAC scenario in compensating effectively all the local and inter-area oscillations. This is further validated through the Prony analysis results of Table II, which shows that only the inter-area compensation has slightly been affected.

TABLE III

INSTRUMENT TRANSFORMER MAXIMUM ERRORS			
Type	**Accuracy Class**	**Max Magnitude Error (%)**	**Max Phase Error (degrees)**
Voltage Transformer	0.5	±0.5	±0.333
Current Transformer	0.5	±0.5	±0.5

PMU STEADY STATE MAXIMUM ERRORS			
Max Voltage Magnitude (%)	**Max Current Magnitude (%)**	**Max Phase Angle (degrees)**	**Max Frequency (Hz)**
±0.02	±0.03	±0.57	±0.005

PMU MAXIMUM ERRORS UNDER DYNAMIC CONDITIONS					
Signal Type	**Max TVE (%)**	**Magnitude (%)**	**Phase Angle (degrees)**	**Frequency (Hz)**	**Time Interval (s)**
Voltage	12	± 6.2	± 4.58	± 0.3	0.07
Current	3	± 1.6	±1.44255	± 0.3	3

C. Case Study 3: Coherency

Coherency refers to a phenomenon that occurs in power systems where at the event of a contingency, certain generators have similar time-domain behavior, leading that way to the separation of the system into coherent groups. The concept of coherency is especially useful at times where it is desirable to reduce the measurement dependency (and hence the required PMU number) of an application. More specifically, according to the coherent groups obtained during a disturbance, only one PMU can be used at each coherent group (since they have similar responses) in order to derive a common WAC signal for all the generators of the group. As shown in Fig. 1, the application of a 5-cycle three-phase fault on the line connecting bus 2 to bus 3 and the line trip/reconnection followed, results into the separation of the system into four groups. Therefore, the synchronized measurements deriving from only one generator PMU at each group (generators 1, 2, 7 and 10 respectively) are considered in the proposed scheme for estimating the coordination signals. The graphical illustrations (Figs. 5b and 5e) combined with the Prony analysis results (Table II) demonstrate that the coherency concept can be utilized successfully for the reduction of the required PMU measurements and the derived coordination signals without compromising the proposed scheme's performance. Actually, the damping ratios (shown in Table II) resulted from the coherency-based WAC (AdapWAC_Coh) are very close to the ones of the AdapWAC scenario.

D. Case Study 4: Real-time simulation results for generator tripping

Less severe disturbances than faults can also take place in the power system. A common disturbance is the event of a generator trip, which can potentially affect the wide area controller operation since the latter losses an actuator that is coordinated for compensating all the inter-area and local oscillations. Therefore, it is interesting and important to test the performances of all the examined scenarios under the event of a generator trip as well. In particular, in this case study the generator G1 (Fig. 1) trips unexpectedly at t=1s, while dynamic loads exist on same buses as previously (8, 15, 21, 23, 25, 27 and 29). Fig. 5c and 5f depict the *real-time* simulation results of this case study, where it is shown that all the examined scenarios have comparable performances. As it is illustrated

through the Prony analysis results of Table II, the AdapWAC scenario has slightly better performance while the ConvWAC scenario has slightly worst damping ratios compared to all the other scenarios. The latter remark is due to the sensitivity of the ConvWAC scenario in the presence of dynamic loads.

VI. Conclusion

A novel methodology for the coordination of the synchronous generator governor and PSS is proposed to increase the damping capability of the system, especially for compensating the inter-area oscillations. The formulation of the proposed WAC signals becomes feasible by utilizing the multi-machine power system dynamic model, in order to identify and cancel out all the inter-generator interactions. The simultaneous coordination of the governor and PSS is achieved through the interaction of the wide area controller with their common input signal (i.e., rotor speed deviation). Furthermore, this paper presents the development of an adaptive tuning methodology to regulate the contribution of the WAC signals. The proposed adaptive tuning method is based on weights that are calculated through the wide area measurements and the electric connectivity between the generators. Therefore, strongly connected generator pairs will have low weights applied on their respective perturbation terms and conversely, high weights are assigned on the perturbation terms of generator pairs which are connected through weak tie lines. The performances of the proposed governor/PSS coordination and its combination with the adaptive tuning method, is tested through EMT analysis by using the IEEE 39-bus test system, where exponential dynamic load models are assumed in various buses of the system. More specifically, for validation purposes, offline and *real-time* simulations took place, where an OPAL-RT equipment was considered in the case of the latter. Note that the proposed scheme has been tested in the presence/absence of the PSSs. Through the utilization of graphical illustrations and the outcomes of the Prony analysis it can be concluded that the proposed governor/PSS coordination has improved performance compared to the conventional WAC. Even better results are obtained through the use of the adaptive tuning methodology in the proposed WAC scheme, which enhances considerably the power system stability. To evaluate further the performance of the adaptive tuning, realistic measurement errors were considered into the *real-time* simulation. The results have indicated that measurement errors have a very small effect on the proposed scheme's performance. Finally, the coherency concept has been successfully used for reducing the required PMU number as well as the derived WAC signals.

VII. References

[1] M. Jonsson, M. Begovic, and J. Daalder, "A new method suitable for real-time generator coherency determination," *IEEE Trans. Power Systems*, vol. 19, no. 3, pp. 1473-1482, 2004.

[2] X. Wu, F. Dörfler, and M. R. Jovanović, "Input-output analysis and decentralized optimal control of inter-area oscillations in power systems," *IEEE Trans. Power Systems*, vol. 31, no. 3, pp. 2434-2444, 2016.

[3] A. R. Messina, Inter-area Oscillations in Power Systems: A Nonlinear and Nonstationary Perspective (Power Electronics and Power Systems), Guadalajara: Springer, 2009.

[4] M. E. Raoufat, K. Tomsovic, and S. M. Djouadi, "Virtual actuators for wide-area damping control of power systems," *IEEE Trans. Power Systems*, vol. 31, no. 6, pp. 4703-4711, 2016.

[5] S. Mohagheghi, G. Venayagamoorthy, and R. Harley, "Optimal wide area controller and state predictor for a power system," *IEEE Trans. Power Systems*, vol. 22, no. 2, pp. 693-705, 2007.

[6] J. Giri, "Proactive management of the future grid," *IEEE Power and Energy Technology Systems Journal*, vol. 2, no. 2, pp. 43-52, 2015.

[7] D. Roberson and J. F. O'Brien, "Loop shaping of a wide-area damping controller using HVDC," *IEEE Trans. Power Systems*, vol. 32, no. 3, pp. 2354-2361, 2017.

[8] M. Mokhtari and F. Aminifar, "Toward wide-area oscillation control through doubly-fed induction generator wind farms," *IEEE Trans. Power Systems*, vol. 29, no. 6, pp. 2985-2992, 2014.

[9] L. Zacharia, L. Hadjidemetriou, and E. Kyriakides, "Integration of renewables into the wide area control scheme for damping power oscillations," *IEEE Trans. Power Systems*, vol. 33, no. 5, pp. 5778-5786, 2018.

[10] T. Surinkaew and I. Ngamroo, "Hierarchical co-ordinated wide area and local controls of DFIG wind turbine and PSS for robust power oscillation damping," *IEEE Trans. Sustainable Energy*, vol. 7, no. 3, pp. 943-955, July 2016.

[11] R. Yousefian, R. Bhattarai, and S. Kamalasdan, "Transient stability enhancement of power grid with integrated wide-area control of wind farms and synchronous generators," *IEEE Trans. Power Systems*, vol. 32, no. 6, pp. 4818-4831, 2017.

[12] D. Dotta, A. S. e Silva, and I. C. Decker, "Wide-area measurements-based two-level control design considering signal transmission delay," *IEEE Trans. on Power Systems*, vol. 24, no. 1, pp. 208-216, 2009.

[13] A. Thakallapelli, S. J. Hossain, and S. Kamalasadan, "Coherency and online signal selection based wide area control of wind integrated power grid," *IEEE Trans. on Industry Applications*, vol. 54, no. 4, pp. 3712-3722, 2018.

[14] Y. Liu, S. You, and Y. Liu, "Study of wind and PV frequency control in U.S. power grids—EI and TI case studies," *IEEE Power and Energy Technology Systems Journal*, vol. 4, no. 3, pp. 65-73, 2017.

[15] F. Okou, L.-A. Dessaint, and O. Akhrif, "Power system stability enhancement using a wide area signals based hierarchical controller," *IEEE Trans. Power Systems*, vol. 20, no. 3, pp. 1465-1477, Aug. 2005.

[16] A. E. Leon and J. A. Solsona, "Power oscillation damping improvement by adding multiple wind farms to wide-area coordinating controls," *IEEE Trans. Power Systems*, vol. 29, no. 3, pp. 1356-1364, 2014.

[17] Y. Xu, F. Li, Z. Jin, and M. Hassani Variani, "Dynamic gain-tuning control (DGTC) approach for AGC with effects of wind power," *IEEE Trans. Power Syst.*, vol. 31, no. 5, pp. 3339-3348, 2016.

[18] D. Apostolopoulou, P. W. Sauer, and A. D. Domínguez-García, "Balancing authority area model and its application to the design of adaptive AGC systems," *IEEE Trans. Power Systems*, vol. 31, no. 5, pp. 3756-3764, 2016.

[19] L. Zacharia, M. Asprou, and E. Kyriakides, "Measurement errors and delays on wide-area control based on IEEE std C37.118.1-2011: impact and compensation," *IEEE Systems Journal (Early Access).*

[20] G. C. Zweigle and V. Venkatasubramanian, "Wide-area optimal control of electric power systems with application to transient stability for higher order contingencies," *IEEE Trans. Power Systems*, vol. 28, no. 3, pp. 2313-2320, 2013.

[21] E. Ghahremani and I. Kamwa, "Local and wide-area PMU-based decentralized dynamic state estimation in multi-machine power systems," *IEEE Trans. Power Systems*, vol. 31, no. 1, pp. 547-562, 2016.

[22] P. W. Sauer and M. A. Pai, Power System Dynamics and Stability, Prentice Hall, 1998.

[23] M. Eremia and M. Shahidehpour, Handbook of Electrical Power System Dynamics, Wiley-IEEE Press, 2013.

[24] P. M. Anderson and A. A. Fouad, Power System Control and Stability, 2nd Edition, Wiley-IEEE Press, 2002.

[25] D. Karissson and D. J. Hill, "Modelling and identification of nonlinear dynamic loads in power systems," *IEEE Trans. Power Systems*, vol. 9, no. 1, pp. 157-166, 1994.

[26] P. Ju, E. Handschin, and D. Karlsson, "Nonlinear dynamic load modelling: model and parameter estimation," *IEEE Trans. on Power Systems*, vol. 11, no. 4, pp. 1689-1697, 1996.

[27] ENTSO-E, "Analysis of CE inter-area oscillations of 1st December 2016," ENTSO-E, Brussels, 2017.

[28] V. S. Patel, F. S. Bhil, F. S. Kazi, and S. R. Wagh, "Energy-sorted Prony analysis for identification of dominant low frequency oscillations," in *Proc. Australian Control Conference*, Fremantle, 2013.

[29] D. P. Wadduwage, U. D. Annakkage, and K. Narendra, "Identification of dominant low-frequency modes in ring-down oscillations using multiple Prony models," *IET Gener. Transm. Distrib.*, vol. 15, no. 9, pp. 2206-2214, 2015.

[30] "IEEE standard for synchrophasor measurements for power systems, Amendment 1: Modification of selected performance requirements, IEEE Std C37.118.1a™-2014," IEEE Power and Energy Society, NY, USA, 2014.

VIII. BIOGRAPHIES

Lazaros Zacharia (S'15) obtained the BSc in Electrical and Computer Engineering from the National Technical University of Athens, Greece, in 2013. In 2014, he obtained the MSc in Sustainable Energy Futures with distinction from Imperial College, London. He is currently a Ph.D. student in the Department of Electrical and Computer Engineering at the University of Cyprus and a Researcher at the KIOS Research and Innovation Center of Excellence. His research interests lie in the areas of Wide Area Monitoring and Control, power systems dynamics and stability, smart grids and renewables.

Markos Asprou (S'09, M'15) received the B.Sc and Ph.D. degree in Electrical Engineering from the University of Cyprus, in 2009 and 2015 respectively. He is currently a Research Associate at the KIOS Research and Innovation Center of Excellence of the University of Cyprus. His research interests include monitoring and state estimation of power systems using synchronized measurements, estimation of transmission line parameters, transient stability, and wide area monitoring and control of power systems.

Elias Kyriakides (S'00, M'04, SM'09) received the B.Sc. degree from the Illinois Institute of Technology in Chicago, Illinois in 2000, and the M.Sc. and Ph.D. degrees from Arizona State University in Tempe, Arizona in 2001 and 2003 respectively, all in Electrical Engineering. He is currently an Associate Professor in the Department of Electrical and Computer Engineering at the University of Cyprus, and a founding member of the KIOS Research and Innovation Center of Excellence. He served as the Action Chair of the ESF-COST Action IC0806 "Intelligent Monitoring, Control, and Security of Critical Infrastructure Systems" (IntelliCIS) (2009-2013). He is an Associate Editor of the IEEE Systems Journal and an Editor of the IEEE Transactions on Sustainable Energy. His research interests include wide area monitoring and control of power systems, the optimization of power system operation techniques, and the integration of renewable energy sources.